Supporting information for:

Shaping reactor microbiomes to produce the fuel precursor *n*-butyrate from pretreated cellulosic hydrolysate

Matthew T. Agler[1], Jeffrey J. Werner[1,2], Loren B. Iten[2], Arjan Dekker[1],

Michael A. Cotta[3], Bruce S. Dien[3], and Largus T. Angenent[1*]

[1] Department of Biological and Environmental Engineering, Cornell University, Ithaca, NY 14853

[2] Chemistry Department, SUNY Cortland, Bowers Hall, PO Box 2000, Cortland, NY 13045

[3] United States Department of Agriculture, Agricultural Research Service, Peoria, IL 61604

* Author to whom correspondence should be sent (la249@cornell.edu)

The supporting information is organized as follows:

S.1: Operation of a bioreactor with unpretreated corn fiber as substrate
S.2: Analysis of the effluent carbohydrates of R_{base}
S.3: Startup of R_{acid}, R_{base}, and R_{heat}
S.4: OTU network analysis
S.5: Batch test results for lactate as an intermediate to *n*-butyrate
S.6: The interplay of primary and secondary fermentation reactions

Figure S1: Influent and effluent COD composition and effluent soluble carbohydrates for R_{acid}, R_{base}, and R_{heat}
Figure S2: Biological hydrolysis in R_{acid}, R_{base}, and R_{heat}
Figure S3: Principal coordinates of weighted UniFrac distances, with each Period denoted
Figure S4: Principal component analysis and evenness of microbial communities of R_{acid}-R_{heat}
Figure S5: 48-hour cycle analysis for R_{acid}, R_{base}, and R_{heat}
Figure S6: Rates of *n*-caproate formation are correlated with relative abundance of the genus *Thermosinus*

Supporting experimental methods and results

Table S1: Pretreatment
Table S2: Operating conditions
Table S3: Performance

Supporting Information

S.1 Operation of a bioreactor with unpreatreated corn fiber as substrate

We operated a fourth bioreactor for 100 days to convert unpretreated corn fiber to *n*-butyrate. We discontinued operation because the unpretreated pericarp (corn-kernel shell) fraction of the biomass was hydrophobic in nature, which caused poor degradation and mixing. Indeed, by day 90 of the operating period, total product formation rates in this reactor were only 50-60% of the levels of the other reactors. Besides hydrophobicity problems, the volatile solids (VS) loading rate in this reactor was 120-130% higher than for the other reactors due to the absence of pretreatment, and this combined with low productivity resulted in excessive buildup of solids in the bioreactor. We determined by day 100 that further operation was unsustainable and stopped operating that reactor.

S.2: Analysis of the effluent carbohydrates of R_{base}

The dilute-alkali pretreatment solubilized more COD than the hot-water pretreatment (Table 1, main text), but we discovered that the soluble fraction of the hydrolysate was mostly composed of polysaccharides that were inefficiently degraded in R_{base}, resulting in soluble carbohydrates in the effluent (Figure S1). We analyzed the effluent carbohydrates from R_{base} via HPLC, which revealed that the peak retention was close to that of other polysaccharides (slightly earlier than cellobiose) and that it had the same retention time and shape as a xylan standard. Although we did not perform techniques to identify the effluent carbohydrates with

100% certainty, xylan is the probable carbohydrate polymer because corn fiber is composed mostly of hemicellulose (Table S1).

S.3: Startup of R_{acid}, R_{base}, and R_{heat}

We inoculated four bioreactors and immediately began an acidic pH regime (pH 5.5) to inhibit methanogens and promote *n*-butyrate metabolism. During the immediate startup period, significant methane partial pressures were observed (e.g., 30-45% of biogas on day 13), but these decreased below detection by day 125 of the operating period in reactors fed dilute-acid and dilute-alkaline pretreated substrates (R_{acid} and R_{base}, respectively) and by day 97 in the reactor fed hot-water pretreated substrate (R_{heat}). By day 120 of the operating period, production of major short-chain carboxylates (acetate, *n*-butyrate, and *n*-caproate) became stable. The biogas hydrogen composition and effluent TCOD and SCOD had also stabilized in all three of the reactors (Figure S1). The distribution of bacterial phylotypes in all of the bioreactor communities became very uneven during startup (Figure S4C). Simultaneously, the phylogenetic structure of the reactor bacterial communities, measured using weighted UniFrac [1], diverged from the inoculum, and each reactor community was identifiably unique after ~50 days (Figure S4 A, B).

S.4: OTU network analysis

We probed potential metabolic groupings of OTUs by building a network based on OTU correlations. First, we narrowed all of the 1063 OTUs to create a more manageable list and to get rid of OTUs with very low abundance. We removed OTUs with < 30 total

reads and OTUs that appeared in $\leq 10\%$ of samples (i.e., ≤ 7 samples). Because our microbiomes were relatively uneven, these restrictions resulted in only 52 OTUs. We used the correlation calculating function in R 2.13.2 (see reference in main text) to calculate the Pearson's correlation matrix and significance of the correlations of each OTU with every other OTU. We considered a correlation coefficient (r) to be significant if $|r| > 0.5$ and $p \leq 0.01$. Next, we used Cytoscape 2.8.0 (see reference in main text) to create a visualization of the network where nodes were OTUs and edges were correlations (solid if the correlation was positive, dashed if it was negative). We scaled the nodes by their highest relative abundance in any sample. Edges were weighted by the strength of the correlation (the value of $|r|$).

S.5: Batch test results for lactate as an intermediate to n-*butyrate*

We directly tested the potential for lactate production and the coupling of lactate oxidation with acetate reduction to *n*-butyrate in batch fermentations with mixed liquor from R_{acid}. First, we performed batch fermentations of cellobiose (a common biological degradation product of cellulose) at conditions similar to R_{acid}. In 44-h fermentations with 10mM cellobiose, most of the cellobiose carbon ended up in glucose (21%) or lactate (48%) and the pH fell to 5.0, inhibiting further conversion (neither glucose nor lactate were detected in control batches with no cellobiose). In separate batch experiments we tested for lactate conversion to *n*-butyrate (via coupled oxidation of lactate with acetate reduction to *n*-butyrate) by adding 15mM or 30mM L-lactate to triplicate batch fermentations (with a control set without L-lactate). Indeed, while the control triplicate formed negligible amounts of *n*-

butyrate, the triplicate with 15 mM L-lactate as substrate produced 2.88±0.84 mM

n-butyrate and consumed 1.30±0.75 mM acetate in 3 days. The triplicate with

30mM L-lactate produced only 2.31±1.42 mM *n*-butyrate and consumed 1.06±1.16

mM acetate. In both cases the stoichiometry is ~2.2 *n*-butyrate per acetate, while

estimates in literature are ~1.5-1.75 [2,3]. The low rates compared to the observed

lactate utilization rates during the cycle analysis could be either due to absence of

some nutrient that was available in the pretreated biomass, or due to oxygen

intrusion during transfer of the effluent to batch bottles, or due to the fact that we

only added L-lactate, while D-lactate may have been the available compound in the

reactors.

S.6: The interplay of primary and secondary fermentation reactions

To study the presence of secondary fermentation pathways, we performed: 1. batch

experiments with mixed liquor from R_{acid} at thermophilic conditions (supporting

information); and 2. cycle analysis during which we monitored metabolites in R_{acid}, R_{base},

and R_{heat} throughout a 48-h period (between two feedings). For the latter analysis, we

report specificities of acetate, *n*-butyrate, and *n*-caproate throughout the cycle period to

identify accumulation of intermediate products as peaks and their dynamic behaviors

(Figure S5). Our batch experiment and cycle analysis showed that lactate was an

important intermediate product from primary fermentation in R_{acid} (1.67 mM at 19 h in

Figure S5A). The coupling of lactate oxidation and acetate reduction produces *n*-butyrate

(lactate + acetate → *n*-butyrate) in cow rumen as a secondary fermentation pathway [4,5].

The simultaneous decreases in lactate and acetate specificity (Figure S5A) and

conversion of acetate and lactate to n-butyrate in the batch tests show that this secondary fermentation pathway to generate *n*-butyrate was occurring. That we only observed a modest increase in *n*-butyrate specificity as a result, can be explained by our observation of a distinct and temporary increase in *n*-caproate specificity with a peak around 28 h for R_{acid} (Figure S5A). This phenomenon indicates the existence of a hereto-unknown secondary fermentation pathway (lactate + *n*-butyrate → *n*-caproate) under thermophilic conditions. The other known possible secondary fermentation pathway to produce *n*-caproate, which occurs through the coupling of ethanol oxidation and *n*-butyrate reduction (ethanol + *n*-butyrate → *n*-caproate) [5, 6], did not occur in our thermophilic bioreactor studies even after many repeated trials over a two-year period (data not shown).

Even though no lactate accumulated in R_{base}, a peak in the *n*-caproate specificity within the 48-h cycle suggests that secondary fermentation also occurred in this bioreactor (Figure S5B). We did observe lactate accumulation (0.68 mM at 5.5 h in Figure S5C) during the cycle analysis for R_{heat}, and removal of lactate concurrent with increases in both *n*-butyrate specificity and *n*-caproate specificity similar to R_{acid} (Figure S5C). This result showed that both secondary fermentation pathways -- lactate + acetate → *n*-butyrate and lactate + *n*-butyrate → *n*-caproate -- played important roles along with primary fermentation in producing *n*-butyrate. However, we did not perform flux analyses to determine the relative importance for each of these pathways. The absence of lactate accumulation and the highest concentrations of *n*-caproate were indicative that conversion of *n*-butyrate into *n*-caproate was more important in R_{heat} than R_{acid} and R_{base}. For optimization of the *n*-butyrate specificity, however, this secondary fermentation

pathway is disadvantageous and should be repressed. The secondary fermentation pathways that we observed in our bioreactors had been described for rumen only [2, 7, 8]. Our results suggest that future bioreactor studies and mathematical efforts should also focus on secondary fermentation pathways because they clearly affected the specificity of the product spectrum for the carboxylate platform.

Figure S1: Influent and Effluent COD composition and effluent soluble carbohydrates for R_{acid}, R_{base}, and R_{heat}
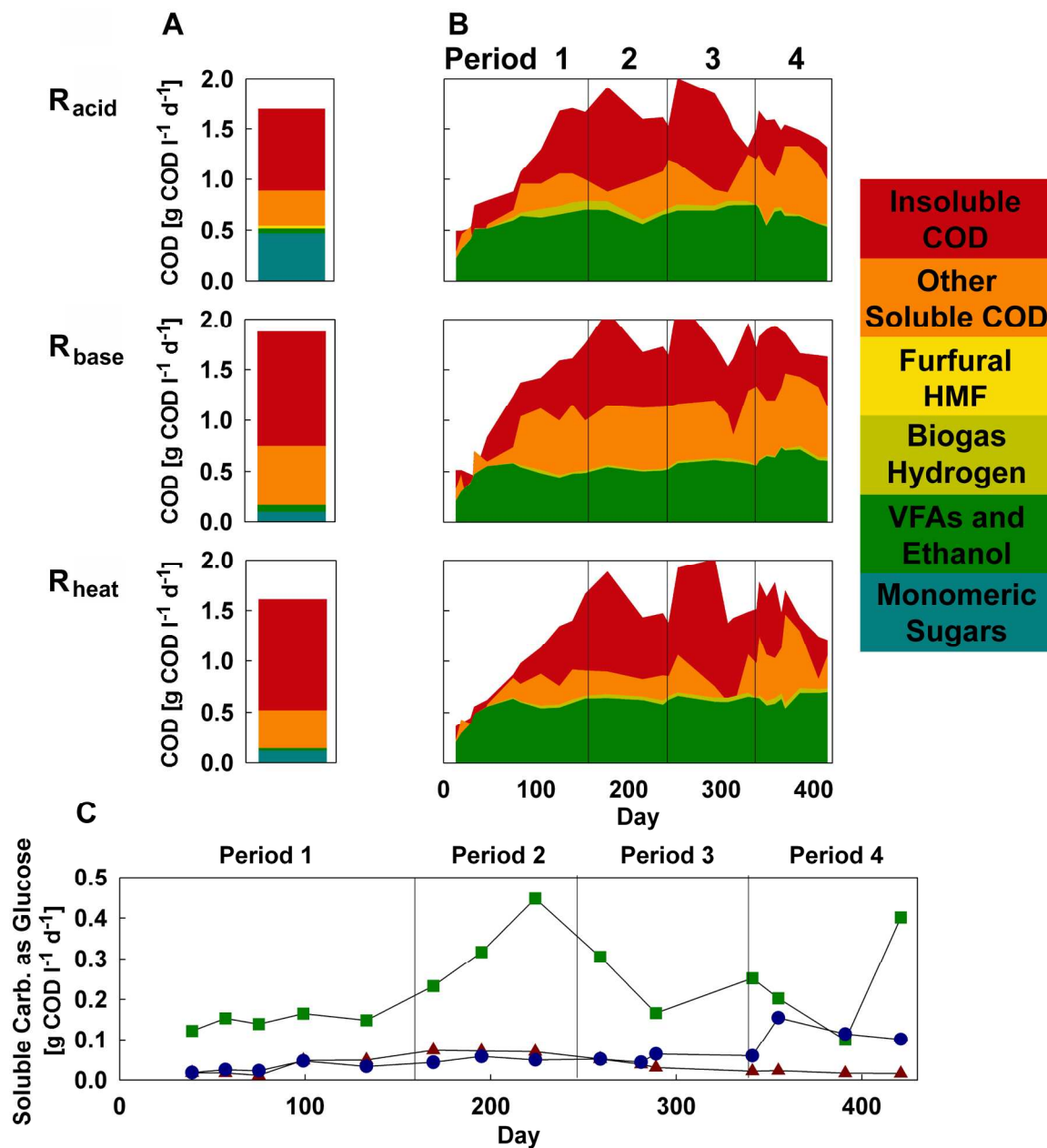

Figure S1. COD composition in substrate and effluent for R_{acid}, R_{base}, and R_{heat}. A. Composition of COD in the dilute-acid, dilute-alkaline, and hot-water pretreated corn fiber hydrolysates; B. Composition of COD in the R_{acid}, R_{base}, and R_{heat} effluents; and C. Soluble carbohydrates in the effluent of R_{acid}, R_{base}, and R_{heat}, where red triangles are R_{acid}, green squares are R_{base}, and blue circles are R_{heat}.
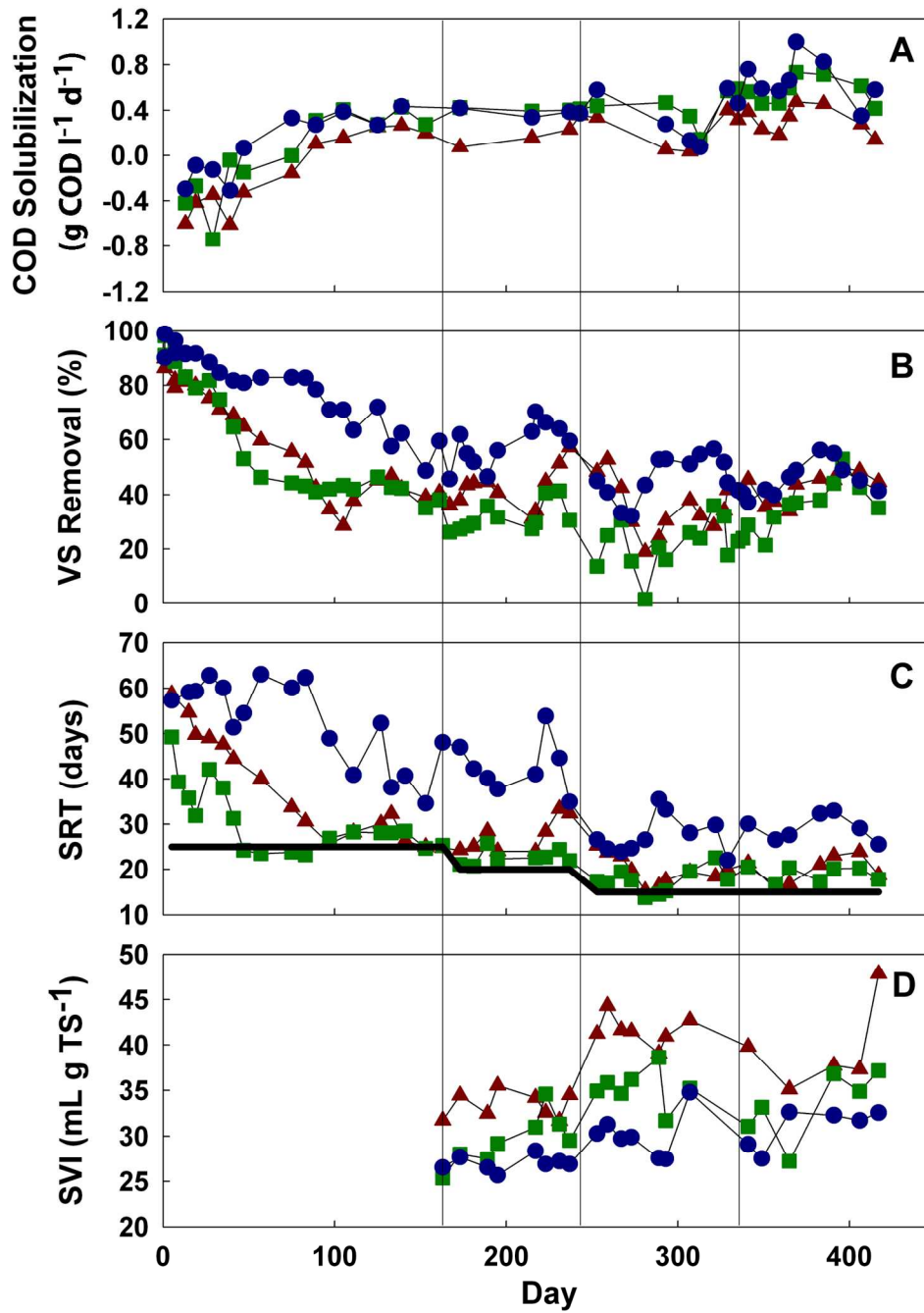
Figure S2. Biological solids hydrolysis

Figure S2. R_{heat} was the most efficient at biological hydrolysis of solid substrate due to the best settling biomass. Red triangles are R_{acid}, green squares are R_{base}, and blue circles are R_{heat}; A. Rate of solubilization of particulate COD; B. Percent VS destruction during conversion to *n*-butyrate; C. SRT for R_{acid}, R_{base}, and R_{heat}. The black line indicates the hydraulic retention time for comparison; and D. SVI for the mixed liquor of the reactors, only measured in Period 2 - 4. A higher SVI indicates a relatively poorer settling sludge, and values are normalized for total solids content of the sludge.

Figure S3: Principal coordinates of weighted UniFrac distances, with each Period denoted
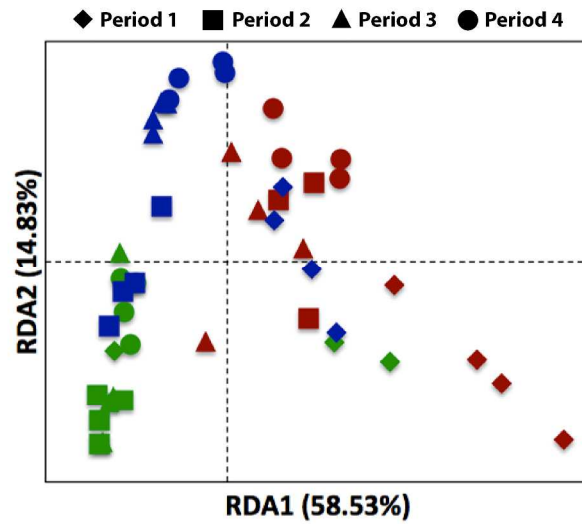

Figure S3. Principal coordinates decomposition of weighted UniFrac between-sample community distances. Same data as in Figure 3A, except that sample points are shaped by period. Red: R_{acid}, Green: R_{base}, and Blue: R_{heat}.

Figure S4: Principal component analysis and evenness of microbial communities of R_{acid}, R_{base}, and R_{heat}
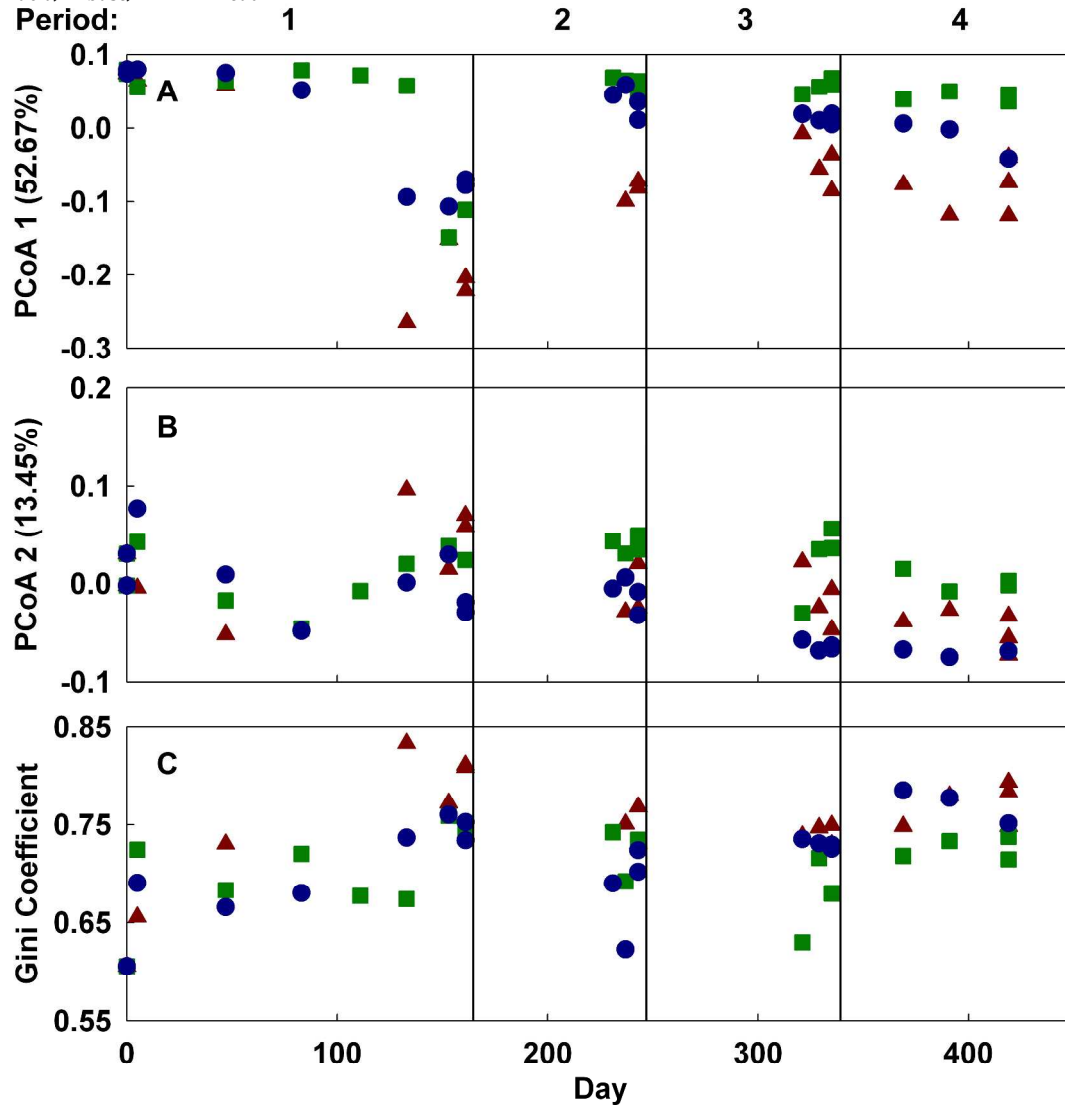
Figure S4. Bacterial community information for R_{acid}, R_{base}, and R_{heat} during the operating period, where red triangles are R_{acid}, green squares are R_{base}, and blue circles are R_{heat}; A. Weighted UniFrac principal coordinate 1 describes 52.67% of community phylogenetic variation; B. Weighted UniFrac principal coordinate 2 describes 13.45% of community phylogenetic variation; and C. Evenness of the bacterial community, described by the Gini coefficient where 0 is a completely even community and 1 is a community dominated by only one phylotype.

Figure S5: 48-hour cycle analysis for R_{acid}, R_{base}, and R_{heat}
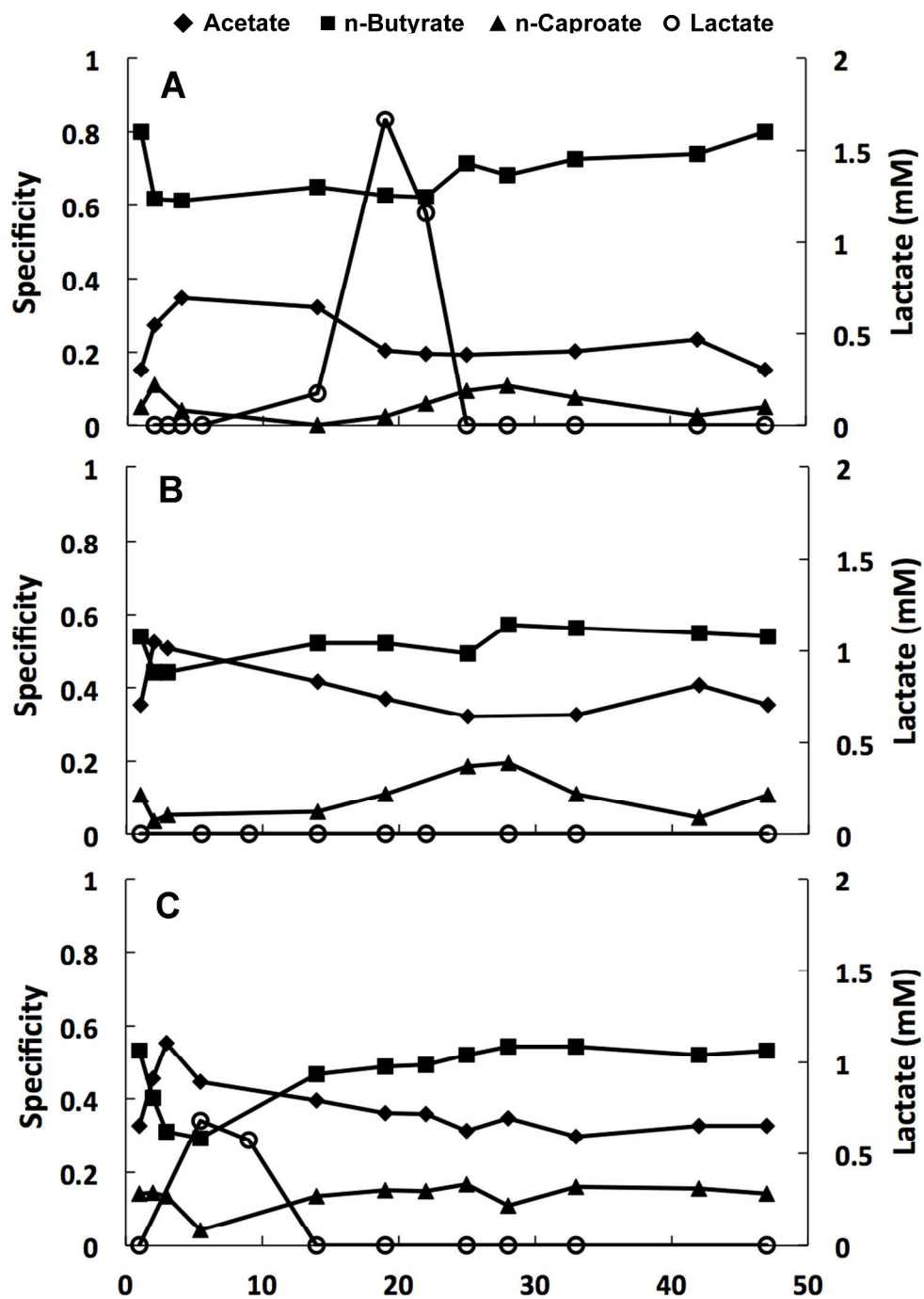

Figure S5. 48-hour cycle analysis demonstrates the dynamic relationship between intermediate lactate and the acetate, *n*-butyrate, or *n*-caproate specificities (i.e., ratio of specific product in COD to all fermentation products in COD) in R_{acid} (A), R_{base} (B), and R_{heat} (C).

Figure S6: Rates of n-*caproate formation are correlated with relative abundance of the genus* Thermosinus
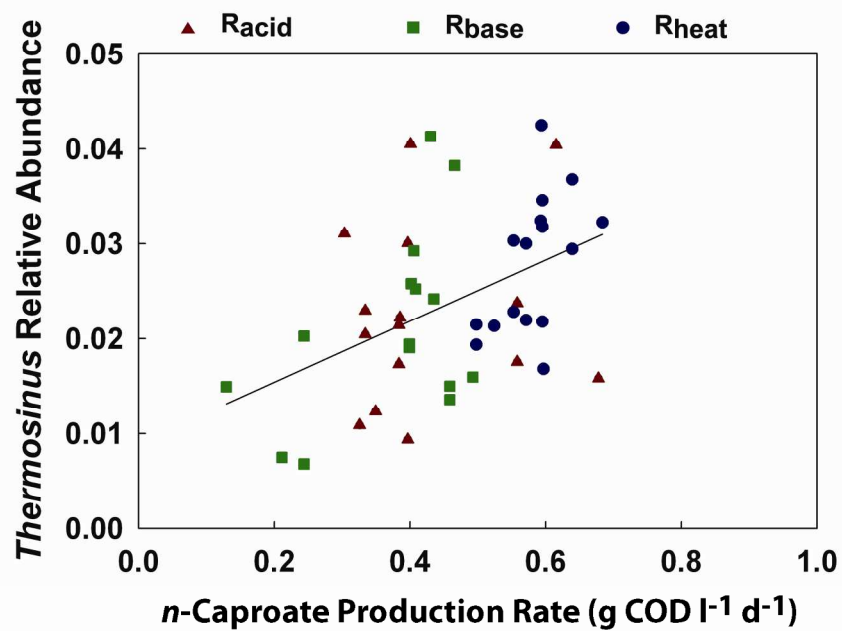

Figure S6. Rates of *n*-caproate production are correlated with relative abundance of the genus *Thermosinus* across R_{acid}, R_{base}, and R_{heat} ($R^2 = 0.21$).

Supporting Experimental Methods

Corn fiber pretreatment

Corn fiber pretreatment was performed at the USDA Agricultural Research Service in Peoria, IL, USA. 150 g of corn fiber, which was received at ~45% solids content was mixed into a 316 stainless steel tube reactor with 320 ml of either dilute acid solution (0.5% w/w sulfuric acid), lime solution (1:10 $Ca(OH)_2$ to dry biomass), or distilled water. The reactors were incubated at $160^{o}C$ for 20 min in a fluidized-sand heating bath. At the end of a 20-min operating period, the reactors were immediately quenched in water. The reactor contents were subsequently transferred to shipping buckets and the reactors rinsed with 700 ml of distilled water, so that the concentration of total solids added to water was ~66 g l^{-1}. The buckets were shipped at $4^{o}C$ to Cornell University for anaerobic treatment and were frozen upon arrival, after mixing all buckets in a large container to assure homogeneity. The *unpretreated* substrate was prepared at Cornell University by adding 150 g of corn fiber at ~45% solids content to 1 l of distilled water. All substrates were adjusted to pH 5.5 immediately before feeding to reactors by adding HCl or NaOH, as necessary. Table 1 and Table S1 describe the characteristics of the three substrates as measured at Cornell University along with the *unpretreated* substrate. The variation in substrate characteristics was low between prepared batches so the data in Table 1 and Table S1 are averages over all batches.

Reactor Operation

Identical 5-l reactors were designed to convert pretreated or *unpretreated* corn fiber to *n*-butyrate. The reactors were anaerobic sequencing batch reactors (ASBRs), designed to settle for one hour before drawing effluent to increase the solids retention times (SRT) compared to the hydraulic retention time (HRT). The reactors were timed to mix once per hour by biogas recirculation with a standard drive pump system (Masterflex, Cole-Parmer Instrument Company, Vernon Hills, IL). All reactors were controlled at pH = 5.5 with a pH controller/transmitter (Euteach Instruments pH 800, Thermo Scientific, Vernon Hills, IL), connected to fixed-speed drives (Masterflex) for automatic addition of 5M HCl or NaOH. The acid and base pumps shared a power source with the recirculation pumps so that addition of acid or base was only possible when the reactors were actively being mixed by gas recirculation. The reactors were temperature controlled at $55 \pm 1 {}^{o}C$ with water circulated through an external heating jacket with a heating recirculator (PolyScience, Inc., Niles, IL). The biogas collection system included a manometer-style pressure control system in which one bottle that was open to the reactor was connected via acidified water (to prevent microbial growth) to a second bottle that was open to the atmosphere. This insured that pressure inside the reactor would not drop below atmospheric pressure during drawing off and feeding or due to atmospheric pressure changes. The biogas then flowed through a gas sampling port, a bubbler to prevent air re-entry, and a gas meter (Model 1 l, Actaris Meterfabriek, Delft, The Netherlands)

The reactors were inoculated from a homogenous mix of three sources: 1. The rumen contents of a young sheep, which was strained to remove large fibrous foodstuffs; 2. Sludge from a full-scale thermophilic anaerobic digester treating primary and waste activated sludge (Western Lake Superior Sanitary District, Duluth, MN); and 3. Sludge from a lab-scale batch thermophilic anaerobic digester treating wheat straw. We inoculated with 1 l of inoculum (200 mL rumen fluid, 300 mL batch thermophilic digester, and 500 mL full-scale thermophilic digester sludge), added 4 l of tap water, and allowed five days of acclimation at $55^{o}C$ before commencing feeding. We fed the reactors every other day, resulting in a 48-h cycle consisting of: instant feeding, a 47-h reaction period with intermittent mixing and pH adjustment every h, and a 58-min settling period followed by drawing off effluent (volume equal to the feeding volume) within two min. To compare conversion of corn fiber COD to n-butyrate COD, including any pretreatment losses, we always maintained a total COD loading rate to each bioreactor of 1.92 g COD l^{-1} d^{-1} based on the COD of corn fiber slurry before pretreatment. The VS loading rate was constant, based on VS levels after pretreatment, with 1.01, 1.12, 1.11, and 1.35 g TS l reactor^{-1} d^{-1} for the acid, base, hot water, and *unpretreated* corn fiber, respectively.

Chemical analysis

We used gas chromatography to measure the hydrogen content of the biogas on a Gow-Mac Series 350 TCD gas chromatograph. We determined the soluble constituents of the effluent by filtering with a 0.2-μm nitrocellulose membrane.

Short-chain carboxylate and alcohol levels in the effluent were measured by gas chromatography (HP 5890 Series II) following acidification of filtered samples with 2% formic acid. Effluent soluble carbohydrates were determined colorimetrically by the phenol/sulfuric acid method using a 96-well plate reader (Bio-Tek, Winooski, VT).

Biomass sampling, DNA extraction, and amplification

We always sampled mixed liquor for subsequent sequencing at the end of a 48-hour cycle by first ensuring that the bioreactor was completely mixed, then rapidly collecting a sample from a side port on the bioreactor. The 2-ml biomass aliquots were centrifuged at 10,000 rpm for 10 min, the supernatant was disposed of, and samples were stored at 4°C for up to 4 h before being transferred to -80°C until subsequent processing.

Genomic DNA was extracted from 64 biomass samples using the MoBio PowerSoil 96-well gDNA isolation kit (MoBio Labs, Inc, Carlsbad, CA). DNA was extracted from ~200 mg of biomass according to the MoBio protocol, except that cell lysis was performed by beadbeating. PCR was carried out in triplicate for each sample to amplify 16S RNA genes. We also performed PCR on two water blanks carried through the extraction process. The PCR mastermix utilized 31.25 μl of water, 0.25 μl of 5U μl^{-1} Agilent Easy-A High Fidelity PCR Cloning Enzyme, 5 μl of 10X Easy-A reaction buffer, 1 μl each of 10 μM forward and reverse primers and 10 mM dNTP, 5 μl of 25mM MgCl$_2$, 3 μl of 10 mg ml^{-1} BSA, and 2 μl of sample. The forward primer

combined the 454 primer 'B' and the universal bacterial primer 27F: 5'-GCCTTGCCAGCCCGCTCAGTC**AGAGTTTGATCCTGGCTCAG**-3'. The reverse primer was a concatenation of the 454 primer 'A', followed by a barcode, unique for each sample, followed by the universal bacterial primer 338R: 5'-GCCTCCCTCGCGCCATCAG*XXXXXXXXXXXX***CATGCTGCCTCCCGTAGGAGT**-3'. On each 96-well plate PCR we included three negatives composed of randomly selected reverse primers and no template. Triplicates were pooled with the Mag-Bind EZ Pure magnetic purification kit, and were eluted into 40 ul TE buffer according to the manufacturer's instructions. Pooled triplicates were run on a 1% agarose gel to verify the product. All negatives had no visible band and were not analyzed further. The concentration of dsDNA in each pooled triplicate was measured via fluourometric analysis with the PicoGreen dsDNA quantitation kit (Invitrogen Corp, Carlsbad, CA). The samples were pooled in equimolar amounts into a single sample with a final concentration 19.2 ng μl^{-1} dsDNA. Sequencing was performed on the Roche 454 pyrosequencing platform using Titanium chemistry and beginning sequencing at 454 adaptor A (Engencore, Columbia, SC).

OTU prediction, taxonomy assignment, and OTU table preparation

We used the QIIME 1.2.1 pipeline [9] with default settings to denoise, quality filter, split sequences into the proper samples, and pick OTUs at 97% sequence identity with UCLUST [10]. We aligned sequences to the GreenGenes (GG) core alignment template [11], trimmed to the V1-V2 region of 16S and filtered the alignment with the GG lanemask. We used the bayesian classifier in mothur [12] to assign taxonomy to

OTUs using a 97% ID clustering of the GG database [13]. We determined sample diversity with the Gini coefficient, a measure of the alpha diversity of each sample. The Gini coefficient is essentially unevenness on a scale from 0 to 1. Gini coefficients were calculated from 100 rarefactions of 400 sequences per sample. UniFrac is a beta diversity index that calculates the phylogenetic distance between communities by determining the fraction of phylogeny the communities share [1]. We determined weighted and unweighted UniFrac distances based on 100 rarefactions of the OTU table at 500 sequences per sample. Both weighted and unweighted UniFrac metrics calculate distances between samples based on phylogenetic trees. Unweighted UniFrac considers only presence/absence of an OTU in a given sample (which makes it more affected by uneven communities or low-level contamination), whereas weighted UniFrac weights distances by abundance of each OTU. We only report weighted UniFrac distances here because sample clustering was more informative than with unweighted UniFrac. We used principal coordinate decomposition to graphically display the phylogenetic distances between samples.

Batch tests for lactate as intermediate

To determine if lactate in R_{acid} could originate from glucose and further, from cellobiose, we conducted a 44-h fermentation in triplicate batches designed to resemble conditions in R_{acid}, with effluent from R_{acid} as the inoculum and as the medium. We added 0 or 10mM of cellobiose as substrate. Cellobiose is a glucose dimer, and is a typical product of cellulose degradation by bacterial hydrolytic enzymes. After 44 h, we sampled the bottles, measured the pH, and measured

glucose and lactate accumulation via HPLC and individual short-chain carboxylates and alcohol via GC. To study the feasibility of lactate and acetate conversion to *n*-butyrate, we again designed triplicate batch fermentations set up to resemble conditions in R_{acid} with effluent as inoculum and as medium and with 50mM of MES buffer (pH 5.5). The inoculum already contained 22.3 mM acetate and 32.7 mM *n*-butyrate and we added 0, 15, or 30 mM of L-lactate as substrate. We allowed the fermentation to proceed and sampled the bottles after three days. We measured the levels of acetate, *n*-butyrate, and *n*-caproate in the bottles at the end of the three days.

Table S1: Additional substrate characteristics

Treatment	Hemicellulose (g l⁻¹) [%DM]	Cellulose (g l⁻¹) [%DM]	Lignin (g l⁻¹) [%DM]	HMF (mM)	Furfural (mM)	Succinate [mM]	Lactate [mM]	Acetate [mM]	Acetoin [mM]	Ethanol [mM]
Dilute Acid	0.49 ± 0.04 (n=2) [0.95%]	6.16 ± 0.00 (n=2) [11.90%]	1.19 ± 0.07 (n=2) [2.30%]	1.16 ± 0.25 (n=9)	5.25 ± 0.80 (n=9)	1.06±0.54 (n = 2)	4.22 ± 0 (n = 2)	20.15 ± 3.63 (n = 8)	3.12 ± 0.56 (n=2)	1.81 ± 0.33 (n=6)
Dilute Alkali	3.53 ± 0.07 (n=2) [5.54%]	8.27 ± 0.06 (n=2) [12.98%]	1.08 ± 0.09 (n=2) [1.70%]	0	0.044 ± .064 (n=9)	1.95±0.48 (n=2)	6.05 ± 0.55 (n = 2)	24.18 ± 1.04 (n = 8)	6.30 ± 2.01 (n=2)	1.70 ± .33 (n=6)
Hot Water	3.98 ± 0.07 (n=2) [7.06%]	8.36 ± 0.10 (n=2) [14.83%]	1.30 ± 0.04 (n=2) [2.31%]	0.043 ± .031 (n=9)	0.39 ± 0.21 (n=9)	1.95±0 (n=2)	3.83 ± 0.08 (n = 2)	2.41 ± 1.11 (n = 8)	2.26 ± 1.27 (n=2)	0.40 ± 0.62 (n=6)
None	21.41 ± 0.27 (n=2) [31.95%]	8.36 ± 1.94 (n=2) [12.48%]	2.14 ± 1.81 (n=2) [3.20%]	0	0	NA	NA	NA	NA	NA

n=represents the number of replicate measurements, and the value after ± is the standard deviation. Lignocellulose composition was only measured on one batch of substrate. We measured HMF, Furfural, acetate, and ethanol for each batch of substrate we received (we also measured other short-chain carboxylates but found none). Succinate, lactate, and acetoin were measured only for the first two batches of substrate

Table S2: Operating conditions for Period 1 through Period 4

		Period 1	Period 2	Period 3	Period 4		Before Heat Shock	After Heat Shock
HRT (d)		25	20	15	15		15	15
pH		5.5	5.5	5.5	5.8		5.5	5.5
Substrate Dilution		2x	2.5x	3.33x	3.33x		3.33x	3.33x
VS Loading Rate ($g\ l^{-1}\ d^{-1}$)	R_{acid}	1.01	1.01	1.01	1.01	R_{hisA}	1.01	1.01
	R_{alk}	1.12	1.12	1.12	1.12	R_{hisB}	1.01	1.01
	R_{HW}	1.11	1.11	1.11	1.11			
COD Loading Rate ($g\ COD\ l^{-1}\ d^{-1}$)	R_{acid}	1.69	1.69	1.69	1.69	R_{hisA}	1.69	1.69
	R_{alk}	[1]1.88	[1]1.88	[1]1.88	[1]1.88	R_{hisB}	1.69	1.69
	R_{HW}	1.61	1.61	1.61	1.61			

[1]Standard deviations for the total COD measurement of the substrate were very high, especially for R_{base}, and this value is not statistically higher than R_{acid} or R_{heat} ($p > 0.05$), see Table 1 for standard deviations. The loading rate based on the *unpretreated* biomass is 1.92 g COD $l^{-1}\ d^{-1}$.

Table S3: Bioreactor performance data for R_{acid}, R_{base}, R_{heat}, R_{hisA}, and R_{hisB}

		Period 1	Period 2	Period 3	Period 4		Before Heat Shock	After Heat Shock
Undissociated Carboxylic Acid Concentration (mM)	R_{acid}	22.05 ± 1.72	18.07 ± 0.41	16.07 ± 0.09	6.76 ± 0.25	R_{hisA}	14.17 ± 0.16	13.43 ± 1.21
	R_{base}	19.05 ± 0.30	15.92 ± 0.48	13.91 ± 0.59	7.16 ± 0.41	R_{hisB}	14.33 ± 0.35	14.02 ± 0.69
	R_{heat}	21.12 ± 1.85	16.63 ± 0.33	14.16 ± 0.87	8.24 ± 0.51			
Fermentation Production Rate (g COD l^{-1} d^{-1})	R_{acid}	0.644 ± 0.033	0.662 ± 0.010	0.744 ± 0.004	0.540 ± 0.020	R_{hisA}	0.696 ± 0.002	0.693 ± 0.013
	R_{base}	0.481 ± 0.005	0.511 ± 0.015	0.586 ± 0.023	0.590 ± 0.032	R_{hisB}	0.703 ± 0.031	0.685 ± 0.023
	R_{heat}	0.546 ± 0.043	0.591 ± 0.027	0.641 ± 0.027	0.671 ± 0.042			
n-Butyrate Production Rate (g COD l^{-1} d^{-1})	R_{acid}	0.352 ± 0.009	0.395 ± 0.013	0.440 ± 0.005	0.273 ± 0.027	R_{hisA}	0.481 ± 0.006	0.471 ± 0.028
	R_{base}	0.197 ± 0.017	0.201 ± 0.011	0.253 ± 0.030	0.255 ± 0.006	R_{hisB}	0.510 ± 0.002	0.481 ± 0.002
	R_{heat}	0.205 ± 0.015	0.261 ± 0.015	0.300 ± 0.030	0.278 ± 0.010			

References:

1.	Lozupone, C.; Knight, R., UniFrac: a new phylogenetic method for comparing microbial communities. *Appl. Environ. Microbiol.* **2005,** *71*, (12), 8228-35.
2.	Duncan, S. H.; Louis, P.; Flint, H. J., Lactate-utilizing bacteria, isolated from human feces, that produce butyrate as a major fermentation product. *Appl. Environ. Microbiol.* **2004,** *70*, (10), 5810-5817.
3.	Diez-Gonzalez, F.; Russell, J.; Hunter, J., The role of an NAD-independent lactate dehydrogenase and acetate in the utilization of lactate by *Clostridium acetobutylicum* strain P262. *Arch. Microbiol.* **1995,** *164*, (1), 36-42.
4.	Counotte, G.; Prins, R., Regulation of lactate metabolism in the rumen. *Vet. Res. Commun.* **1981,** *5*, (1), 101-115.
5.	Agler, M. T.; Wrenn, B. A.; Zinder, S. H.; Angenent, L. T., Waste to bioproduct conversion with undefined mixed cultures: the carboxylate platform. *Trends Biotechnol.* **2011,** *29*, (2), 70-78.
6.	Seedorf, H.; Fricke, W. F.; Veith, B.; Bruggemann, H.; Liesegang, H.; Strittmatter, A.; Miethke, M.; Buckel, W.; Hinderberger, J.; Li, F.; Hagemeier, C.; Thauer, R. K.; Gottschalk, G., The genome of *Clostridium kluyveri*, a strict anaerobe with unique metabolic features. *Proc. Natl. Acad. Sci. U.S.A.* **2008,** *105*, (6), 2128-33.
7.	Belenguer, A.; Duncan, S. H.; Holtrop, G.; Anderson, S. E.; Lobley, G. E.; Flint, H. J., Impact of pH on Lactate Formation and Utilization by Human Fecal Microbial Communities. *Appl. Environ. Microbiol.* **2007,** *73*, (20), 6526-6533.
8.	Kim, M.; Gomec, C. Y.; Ahn, Y.; Speece, R. E., Hydrolysis and acidogenesis of particulate organic material in mesophilic and thermophilic anaerobic digestion. *Environ. Technol.* **2003,** *24*, (9), 1183 - 1190.
9.	Caporaso, J. G.; Kuczynski, J.; Stombaugh, J.; Bittinger, K.; Bushman, F. D.; Costello, E. K.; Fierer, N.; Pena, A. G.; Goodrich, J. K.; Gordon, J. I.; Huttley, G. A.; Kelley, S. T.; Knights, D.; Koenig, J. E.; Ley, R. E.; Lozupone, C. A.; McDonald, D.; Muegge, B. D.; Pirrung, M.; Reeder, J.; Sevinsky, J. R.; Turnbaugh, P. J.; Walters, W. A.; Widmann, J.; Yatsunenko, T.; Zaneveld, J.; Knight, R., QIIME allows analysis of high-throughput community sequencing data. *Nat. Methods* **2010,** *7*, (5), 335-336.
10.	Edgar, R. C., Search and clustering orders of magnitude faster than BLAST. *Bioinformatics* **2010,** *26*, (19), 2460-2461.
11.	DeSantis, T. Z.; Hugenholtz, P.; Larsen, N.; Rojas, M.; Brodie, E. L.; Keller, K.; Huber, T.; Dalevi, D.; Hu, P.; Andersen, G. L., Greengenes, a chimera-checked 16S rRNA gene database and workbench compatible with ARB. *Appl. Environ. Microbiol.* **2006,** *72*, (7), 5069-5072.
12.	Schloss, P. D.; Westcott, S. L.; Ryabin, T.; Hall, J. R.; Hartmann, M.; Hollister, E. B.; Lesniewski, R. A.; Oakley, B. B.; Parks, D. H.; Robinson, C. J.; Sahl, J. W.; Stres, B.; Thallinger, G. G.; Van Horn, D. J.; Weber, C. F., Introducing mothur: Open-source, platform-independent, community-supported software for describing and comparing microbial communities. *Appl. Environ. Microbiol.* **2009,** *75*, (23), 7537-7541.

13.   Werner, J. J.; Koren, O.; Hugenholtz, P.; DeSantis, T. Z.; Walters, W. A.; Caporaso, J. G.; Angenent, L. T.; Knight, R.; Ley, R. E., Impact of training sets on classification of high-throughput bacterial 16S rRNA gene surveys. *ISME J.* **2011,** *6,* (1), 94-103.